ISPRS Journal of Photogrammetry and Remote Sensing 97 (2014) 78–88

Contents lists available at ScienceDirect

ISPRS Journal of Photogrammetry and Remote Sensing

journal homepage: www.elsevier.com/locate/isprsjprs

Modeling diurnal land temperature cycles over Los Angeles using downscaled GOES imagery

Qihao Weng *, Peng Fu

Center for Urban and Environmental Change, Department of Earth and Environmental Systems, Indiana State University, Terre Haute, IN 47809, USA

ARTICLE INFO

Article history:
Received 9 February 2014
Received in revised form 24 June 2014
Accepted 21 August 2014
Available online 16 September 2014

Keywords:
Land surface temperature
Urban heat island
Diurnal temperature cycle
Thermal downscaling
Data fusion
Temporal resolution

ABSTRACT

Land surface temperature is a key parameter for monitoring urban heat islands, assessing heat related risks, and estimating building energy consumption. These environmental issues are characterized by high temporal variability. A possible solution from the remote sensing perspective is to utilize geostationary satellites images, for instance, images from Geostationary Operational Environmental System (GOES) and Meteosat Second Generation (MSG). These satellite systems, however, with coarse spatial but high temporal resolution (sub-hourly imagery at 3–10 km resolution), often limit their usage to meteorological forecasting and global climate modeling. Therefore, how to develop efficient and effective methods to disaggregate these coarse resolution images to a proper scale suitable for regional and local studies need be explored. In this study, we propose a least square support vector machine (LSSVM) method to achieve the goal of downscaling of GOES image data to half-hourly 1-km LSTs by fusing it with MODIS data products and Shuttle Radar Topography Mission (SRTM) digital elevation data. The result of downscaling suggests that the proposed method successfully disaggregated GOES images to half-hourly 1-km LSTs with accuracy of approximately 2.5 K when validated against with MODIS LSTs at the same over-passing time. The synthetic LST datasets were further explored for monitoring of surface urban heat island (UHI) in the Los Angeles region by extracting key diurnal temperature cycle (DTC) parameters. It is found that the datasets and DTC derived parameters were more suitable for monitoring of daytime- other than nighttime-UHI. With the downscaled GOES 1-km LSTs, the diurnal temperature variations can well be characterized. An accuracy of about 2.5 K was achieved in terms of the fitted results at both 1 km and 5 km resolutions.

1. Introduction

Land surface temperature (LST) is a key parameter for investigating surface energy budget (Oke et al., 1992; Friedl, 2002), examining surface urban heat island (SUHI) (Oke, 1982; Streutker, 2003; Weng et al., 2004), and assessing heat-related risks and vulnerability in cities (Harlan et al., 2006; Lafortezza et al., 2009; Buscail et al., 2012). Since these environmental and health issues are characterized by both high spatial and temporal variability, thermal infrared (TIR) data from the existing satellite sensors are not able to characterize effectively these phenomena. Due to technical constraints, the existing sensing systems reflect a tradeoff between temporal and spatial resolution such that the systems with high-spatial resolution possess low-temporal resolution, or vice versa. Currently, no single satellite system can provide TIR data of global coverage that combines both high spatial and temporal resolutions. For a list of major current satellite TIR imaging systems, please refer to Tomlinson et al. (2011). TIR data derived from polar-orbiting satellites possess high to medium spatial resolution but are out-balanced by their long revisit cycles. Geostationary satellites, on the other hand, allow for monitoring of the diurnal cycle of LST because they can scan the Earth's surface in tens of minutes. However, their coarse spatial resolution (usually in the range of 3–5 km) cannot adequately differentiate land cover features. These satellites, therefore, cannot be used to analyze UHI patterns and dynamics and heat-related health risks at the urban neighborhood or community scale. It is highly desirable to explore effective ways to sharpen TIR data and to combine different types of TIR data to generate LSTs at both high temporal and spatial resolutions.

* Corresponding author. Tel.: +1 812 237 2255; fax: +1 812 237 8029.
E-mail address: qweng@indstate.edu (Q. Weng).

http://dx.doi.org/10.1016/j.isprsjprs.2014.08.009
0924-2716/

Existing thermal sharpening techniques basically fall into two categories: spatial and temporal thermal sharpening (Weng et al., 2014). While the spatial sharpening techniques aim at downscaling radiometric surface temperature of a sensor to higher resolutions typically associated with its shorter wavebands (visible and near-infrared) (Guo and Moore, 1998; Kustas et al., 2003; Pu et al., 2006), the temporal sharpening techniques are developed to downscale TIR data from a coarser spatial-resolution but higher temporal-resolution sensor (typically associate with Geostationary satellites) to generate highly temporally resolved LSTs (Gottsche and Olesen 2001; Inamdar et al., 2008; Inamdar and French 2009, Bechtel et al., 2012, Zakšek and Oštir 2012). A classical way for spatial sharpening is to utilize the inverse relationship between LST and NDVI (Kustas et al., 2003; Merlin et al., 2010; Jeganathan et al., 2011). Based on this relationship, Inamdar et al. (2008) and Inamdar and French (2009) employed the MODIS TIR data as a calibration source for GOES TIR data, and further blended the data from the two sensors to generate half-hourly LSTs at 1 km resolution, yielding an accuracy of 2 K. This type of synthetic LST dataset should be very useful for UHI studies, since Rajasekar and Weng (2009) demonstrated that the 1 km MODIS dataset was capable of deriving the UHI intensity, extent, and orientation parameters in Indianapolis by virtue of a non-parametric Gaussian process model. However, it should be noted that LST is a function of many factors, including vegetation abundance and vigor, soil moisture, land cover, topography, and meteorological conditions. Consequently, using NDVI as the only explanatory factor for the spatial and temporal patterns of LST may pose some major problems. More sophisticated models have to be developed by incorporating all key LST associated parameters in the downscaling process.

LSTs derived from geostationary satellites provide a valuable data source for examining thermal spatial landscape patterns and temporal dynamics. Diurnal cycle of LST retrievable from geostationary satellites constitute an important parameter of the Earth's climate system, and the diurnal temperature range (DTR) has been regarded as a meaningful indicator for climate change (Karl et al., 1984; Sun et al., 2006). The diurnal variations of LST are associated with insolation, wind and surface conditions, including land cover, soil moisture, and surface structure (Gottsche and Olesen, 2001). Analyses of diurnal temperature cycle (DTC) by individual land covers have been hampered by the lack of data at appropriate resolutions. Zakšek and Oštir (2012) thus enhanced the spatial resolution of Spinning Enhanced Visible and Infrared Imager (SEVIRI) LSTs over the European region to 1 km resolution using MODIS NDVI, EVI, albedo, emissivity, Corine land cover and elevation as the auxiliary data. Keramitsoglou et al. (2013) developed a method that coupled support vector machine with gradient boosting for downscaling SEVIRI LSTs with MODIS dataset, land cover and digital elevation model as auxiliary data. Although these previous studies have successfully downscaled geostationary TIR data, a detailed analysis of temporal variability of the disaggregated LST data is still lacking. In fact, the multi-temporal characteristic of the geostationary satellites should be an important consideration for the downscaling studies, and such an analysis will undoubtedly facilitate the assessment of the downscaling processes. In this paper, a new method is developed to generate 1-km LST dada by fusing MODIS and GOES datasets. Specific objectives are to explore an efficient and effective way for disaggregating GOES TIR dataset and to analyze the diurnal characteristic of LST in Los Angeles. Least-squares support vector machines is used because of its effectiveness in terms of noise reduction, computation efficiency and accuracy in data generation and fusion (Zheng et al., 2008; Shi et al., 2009). Los Angeles is selected as the study area because this region consists of highly diverse urban fabrics, mix of natural and introduced vegetation, and varying environmental conditions.

2. Study area and data

2.1. Study area

The study area is the Los Angeles (L.A.) County, except for two offshore islands, the Santa Catalina Island and the San Clemente Island (Fig. 1). According to the U.S. census in 2010, it has a population of approximately 10 million, making it the most populous county in the U.S.A. The selected area encompasses geographically diverse land features, ranging from hilly mountains, deep valleys, ocean coastlines, forests, lakes, rivers, brushland and barren land. The primary mountain ranges within the region are Santa Monica Mountains and the San Gabriel Mountains in the southwestern and southeastern parts, respectively. The Mojave Desert begins at the northeastern part of the County and stretches westward. The valleys are largely the population centers, and compose a large percentage of the urban areas. With an average annual precipitation of 15 in., L.A. County possesses a semi-arid Mediterranean climate with a dry summer and a moist winter. The average high temperature is 29 °C in August and 20 °C in January based on the weather records from the Downtown-University of Southern California campus. Temperature experiences apparent change between the inland and coastal areas, as elevation and the distance to the coast increase. Los Angeles has a known problem in air quality, which is related to its UHI phenomenon. According to the Heat Island Group (http://heatisland.lbl.gov/), the heat island effect costs about US $100 million per year in energy.

2.2. GOES imagery data

The GOES system, operated by the United States National Environmental Satellite, Data, and Information Service (NESDIS), continuously scans the continental United States, neighboring environs of the Pacific and Atlantic Oceans, and Central, South America and southern Canada. Currently, the GOES satellites in operation are GOES-12, GOES-13, GOES-14, and GOES-15, located in 60°W, 75°W, 90°W and 135°W, respectively. For the present study, the GOES imagery acquired on January 12, May 12, August 15, and October 15, 2005 (48 images per day) delivered by the GOES-10 Imager was used since they represented downscaling effectiveness in different seasons.

The GOES-10 Imager possesses 5 spectral bands, one visible band at 0.55–0.75 μm, and four infrared bands at 3.8–4 μm, 6.5–7 μm, 10.2–11.2 μm, and 11.5–12.5 μm, respectively. The image data were downloaded through the Comprehensive Large Array-data Stewardship System (CLASS) (http://www.class.ngdc.noaa.gov). During the data pre-processing, the GOES Variable Format counts packaged in Network Common Data Format (netCDF) were first converted to brightness temperature (Weinreb et al., 1997). Specific calibration coefficients for the GOES-10 Imager can be found from the NOAA Satellite and Information Service website (http://www.oso.noaa.gov/goes/goes-calibration/gvar-conversion.htm).

2.3. Auxiliary data

Since LST is strongly influenced by such parameters as solar irradiation, albedo, topography, thermal inertia, and vegetation cover (Weng et al., 2004; Carlson, 2007; Dominguez et al., 2011; Van De Kerchove et al., 2013), this section describes the auxiliary data employed for the downscaling purpose. Both Normalized Difference Vegetation Index (NDVI) and Enhanced Vegetation index (EVI) were utilized in the downscaling scheme. To eliminate the effect caused by clouds, the 16-day composite MODIS vegetation indices (MOD13) at 1 km resolution were adopted.

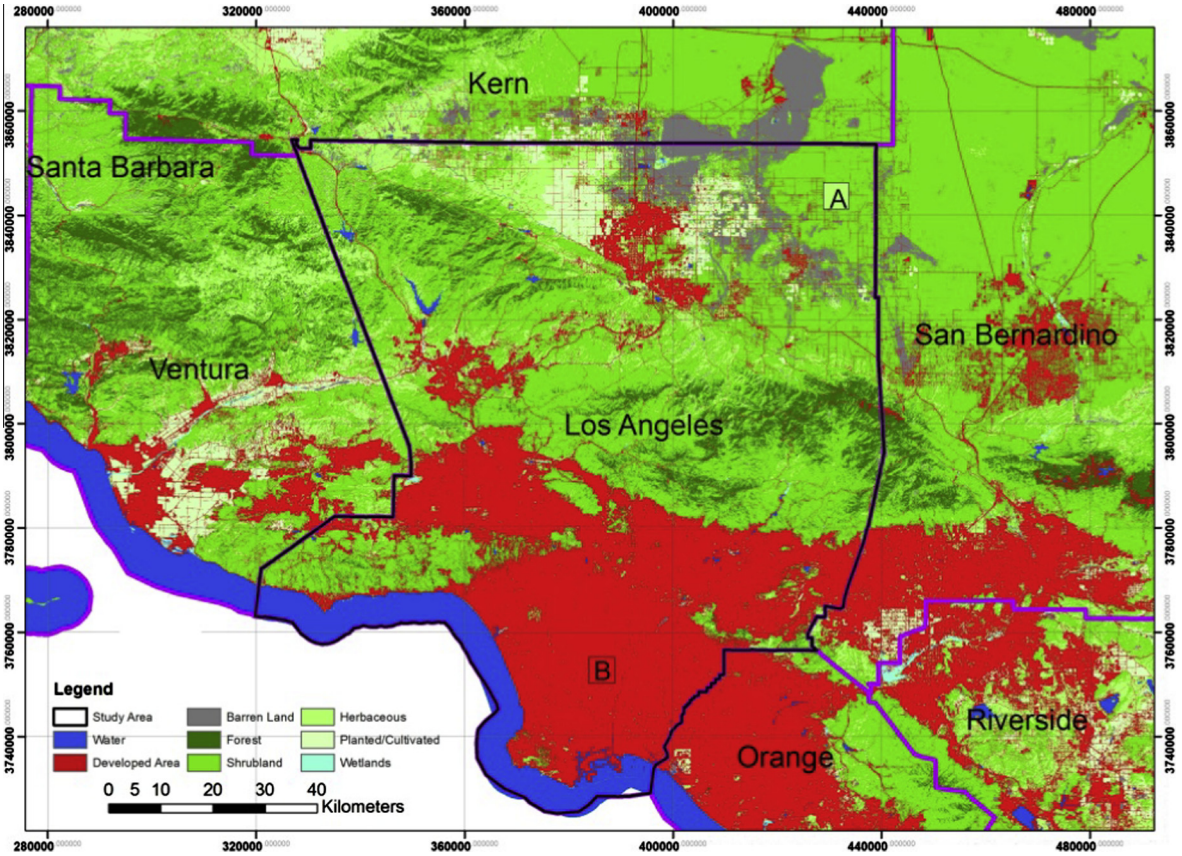

Fig. 1. The study area: Los Angeles County, California, U.S.A. Eight land covers were identified in the National Land Cover Database (2006), including: water, developed area, barren land, forest, shrubland, herbaceous, planted/cultivated, and wetland. Sites A and B, two polygons, both 5 km * 5 km, were selected for the purpose of diurnal temperature modeling.

Another kind of auxiliary data used was land surface albedo. The 8-day composite albedo product (MCD43) from the Terra MODIS measurements was obtained from the Land Processes Distributed Archive Center (LPDAC). The product offered white and black sky albedos in visible, near-infrared, and shortwave bands. The last MODIS data product acquired for use was emissivity, an indicator of the relative capability of land surfaces to emit energy by virtue of radiation. The 8-day average emissivity data was used for two purposes: one for the downscaling procedure, and the other for deriving LST from GOES brightness temperatures, which will be discussed in the next section. In addition, Shuttle Radar Topography Mission (SRTM) digital elevation data was used to aid the downscaling. All the auxiliary datasets were re-projected to the WGS84 UTM coordinate system and resampled with the bilinear interpolation method.

3. Methodology

3.1. Derivation of LST for GOES imagery

Inamdar et al. (2008) developed a procedure to fuse GOES and MODIS LST data that we adapted for this study. Both MODIS LST and emissivity data were first aggregated for every block of 5 by 5 pixels. Cloud-cleared GOES pixels were collocated with the aggregated 5-km MODIS pixels, yielding for each matched domain, a set of GOES brightness temperatures in the TIR channels of 11 μm (T11) and 12 μm (T12) together with the MODIS LST and surface emissivities, ε11 and ε12, in MODIS bands 31 (11 μm) and 32 (12 μm), respectively, with all parameters aggregated to the 5 km domain. Each area sampled by GOES was under a MODIS overpass at least once every day. When accumulated over a period of a month, a sufficiently large sample of matched data pairs to represent the entire domain can be obtained, so as to "calibrate" the GOES brightness temperatures in terms of MODIS-measured LST through the use of a split window scheme, which was then applied to all unmatched cloud-free GOES pixels. The results were half-hourly LST values at 5-km spatial resolution for the entire domain. The split window scheme (Wan and Dozier, 1996) was applied to the GOES TIR channels 4 and 5 to compute LST (Ts) as:

$$\mathrm{Ts} = a_0 + (a_1 + a_2\varepsilon_1 + a_3\varepsilon_2)T_1 + (a_1 + a_4\varepsilon_3 + a_5\varepsilon_4)T_2 \quad (1)$$

where

$$\varepsilon_1 = \frac{1 - (\varepsilon_4 + \varepsilon_5)/2}{(\varepsilon_4 + \varepsilon_5)/2}$$

$$\varepsilon_2 = \frac{\varepsilon_4 - \varepsilon_5}{[(\varepsilon_4 + \varepsilon_5)/2]^2}$$

$$T_1 = (T_4 + T_5)/2$$

$$T_2 = (T_4 - T_5)/2$$

And ε_4 and ε_5 are emissivity values of Channel 4 and 5; T_4 and T_5 brightness temperature values for Channel 4 and 5. Because emissivity data were not available from GOES imagery, MODIS 1-km emissivity data was up-scaled for use to match with the clear-sky GOES pixels that had the same overpass time as MODIS. For this study, we found that the 8-day mean emissivity values can well satisfy the requirement for the data fusion. The original split window algorithm employed angle-dependent regression

coefficients, which changed substantially when the angle was larger than 60° (Wan and Dozier, 1996). This study did not consider the angle-dependency since all the data were within a small viewing angle of less than 30°. Small angles tended not to produce significant LST biases (Wan and Dozier, 1996). A validation procedure comparing LST values up-scaled from MODIS 1-km daily LST measurements with the derived GOES LSTs at the same overpass time indicated that the accuracy of LST derivation from GOES-10 data was 1.8 K (RMSE) with negligible bias.

An important step before the implementation of the split window scheme was cloud screening for GOES pixels. An effective way for identifying cloud contaminated pixels is the Bispectral Threshold and Height (BTH) method (Jedlovec and Laws, 2003), developed at the Global Hydrology and Climate Center. The key to cloud detection in BTH was that emissivity values between 10.7 μm and 3.9 μm of clouds differed from those of land surfaces and oceans so that differences in brightness temperature can be used to differentiate those cloud-contaminated pixels from clear-sky pixels. Half-hourly GOES multi-channel brightness temperatures were first pre-processed. The channels 2 (3.8–4 μm) and 4 (10.2–11.2 μm) were used to produce temperature-difference images, i.e., longwave subtracted by shortwave (channel 4–channel 2). Both the positive differences at nighttime and the negative difference at daytime were preserved in the difference images. Then, two composite images with values closest to zero from the preceding 20 days were created. Additional preceding-20-day composite image was generated for each half-hour using the warmest longwave (10.7 mm) brightness temperature for each location (pixel). This composite image was assumed to represent a warm cloud-free thermal image for each time period. These created images were subject to the tests of adjacent pixel, dimensional spatial variability, minimum difference, and IR threshold (Jedlovec and Laws, 2003), resulting in discrimination of cloud contaminated pixels by using information from local and global spatial and temporal variations.

3.2. Disaggregation of LST to 1-km resolution

Given the complex relationship between LSTs and the auxiliary datasets, simple regression models (e.g., linear regression) may not be able to reveal the causes of the spatial variations in LST. Support vector machines (SVMs), benefiting from the machine learning process such as structural risk minimization, are particular useful in the field of remote sensing due to its ability to handle training datasets (Mantero et al., 2005). For this study, we proposed to use the least square support vector machines (LSSVMs) for the downscaling of GOES LSTs to 1-km resolution, because LSSVM has been found effective in terms of noise reduction, computation efficiency and accuracy in data generation and fusion (Zheng et al., 2008; Shi et al., 2009). LSSVMs are reformulations of the standard SVMs, and are closely related to the regularization networks and Gaussian processes with additional emphasis of primary-dual interpretation (Mountrakis et al., 2011). Specific procedures of LSSVM based LST downscaling included: (1) up-scaling auxiliary datasets (1 km resolution) to match the GOES pixels at 5-km spatial resolution; (2) quantifying the relationship between 5-km auxiliary datasets and GOES LSTs; (3) applying the estimated relationship to the auxiliary datasets at 1 km spatial resolution to derive half-hourly LSTs at 1 km; and (4) validation of the predicted LSTs with observed MODIS LSTs. Fig. 2 shows the detailed procedure for LST downscaling.

3.3. Diurnal temperature cycle (DTC) modeling

Due to the lack of MODIS LST measurements at non-passing times, this study decided to compare DTC modeling results to assess the prediction accuracy for all the downscaled images (48 in total). The DTC model can be used to derive a series of parameters describing the thermal behavior of land surfaces (Gottsche and Olesen, 2001, 2009). Different models have been developed to characterize DTC (Gottsche and Olesen, 2001; Inamdar et al., 2008; Gottsche and Olesen, 2009). Six distinct models were discussed in Duan et al. (2012). We decided to employ the model by Inamdar et al. (2008) to describe the diurnal LST variations because of its better match, which used a harmonic and a hyperbolic decay term for the fitting purpose. The model can be described as a system of equations as follows:

$$T_1(t) = T_0 + T_a \cos\left(\frac{\pi}{\omega}(t - t_m)\right), \quad t < t_s \tag{2}$$

$$T_2(t) = (T_0 + \delta T) + \left[T_a \cos\left(\frac{\pi}{\omega}(t_s - t_m)\right) - \delta T\right] \frac{k}{k + t - t_s}, \quad t \geqslant t_s \tag{3}$$

where, T_0 minimum temperature around sunrise; T_a temperature amplitude; t time (h); ω length of daylight hours (h); t_m time of the maximum (h); t_s start of the nighttime attenuation (h); k attenuation coefficient; $\delta T = T(t \to \infty) - T_0$.

A test site of 5 × 5 pixels from the downscaled GOES 1-km images and the corresponding region of GOES 5-km (only 1 pixel) was selected from shrubland and developed area respectively. Sites A and B in Fig. 1 showed these test sites. The modeling period was limited to between successive sunrises. The Levenberg–Marquardt scheme was utilized to optimize the DTC parameters for the time series LSTs. The attenuation coefficient (k) was determined by constraining the set of Eq. (2) for continuity of first derivatives at the junction point (Inamdar et al., 2008), and the length of daylight hours (ω) was precisely calculated based on astronomical relationships (Gottsche and Olesen, 2001). Next, the model was initiated by providing the initial guess of other five parameters, which led to the convergence of final parameters.

4. Results

4.1. LST downscaling results

GOES images of January 12, May 12, August 12, and October 15 (48 images per day) were downscaled. The clear sky GOES LST pixels screened by the BTH method were input into the LSSVM model to estimate the relationship with the aggregated auxiliary datasets at 5-km resolution. A major consideration in the applicability of SVMs is the choice of kernels. This research tested different kernel functions, including radial basis function (RBF), polynomial function (PF), and linear kernel (LK). It was found that the RBF kernel outperformed over the other two and that predicted LST values were in the typical ranges of land surfaces (250–330 K) (Weng and Fu, 2014). Then, the estimated relationship by LSSVMs was applied to the original auxiliary datasets to predict LSTs at 1 km.

Fig. 3 shows density scatter plots of predicted GOES LSTs at 1 km against MODIS LST measurements at the same overpass time for the four selected days. The mean absolute error for the predicted images was relatively constant, ranging from 1.8 to 2.3 K, indicating that the proposed LSSVM method can disaggregate coarse TIR data to 1 km resolution stably in different months. The correlation coefficients, 0.87, 0.85, 0.80 and 0.84 for the four dates, respectively, further suggested the robustness of the downscaling method. Large values of standard deviation associated with the mean prediction error (2.9 K, 3.0 K, 3.3 K, and 2.9 K, respectively), on the other hand, implied that the downscaling method was not sufficiently robust and should be improved. A possible reason was the incomplete inclusion of explanatory factors to LST variations. For example, soil moisture was not included in this study as an explanatory variable. It has been reported in the

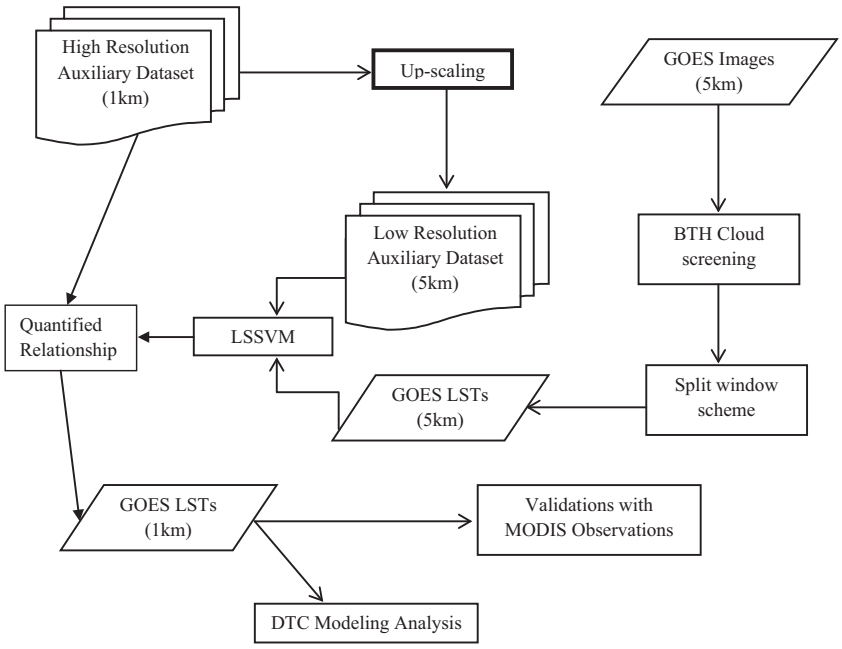

Fig. 2. The procedure for downscaling GOES 5-km image data to generate 1-km LSTs.

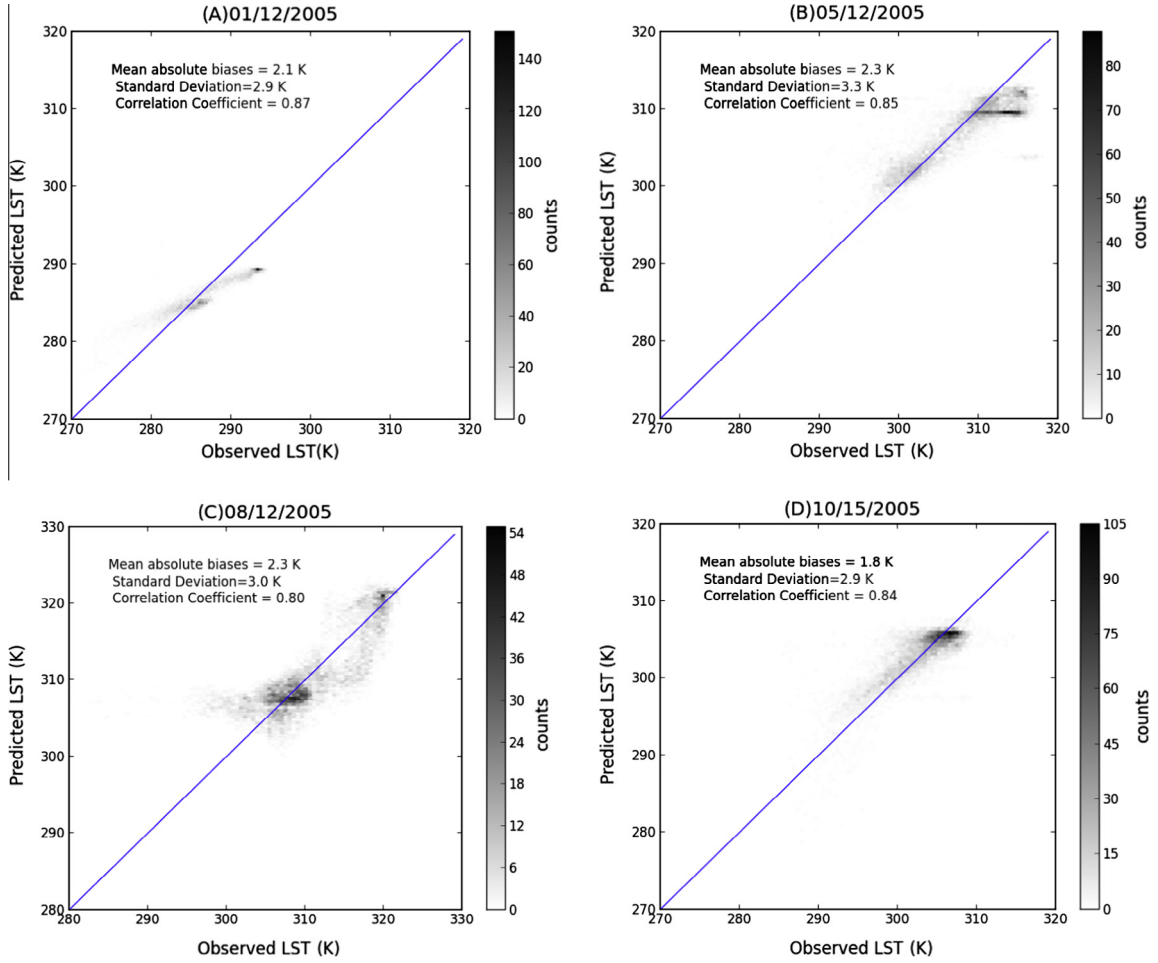

Fig. 3. Validations of predicted GOES LST at 1 km spatial resolution against MODIS LST measurements at the same overpass time on (A) 01/12/2005, (B) 05/12/2005, (C) 08/12/2005, and (D) 10/15/2005.

literature that a small change in soil moisture may lead to a significant change in evapotranspiration and thus impacts to the surface energy budget and LST variations (Owen et al., 1998; Carlson, 2007). However, currently available soil moisture data products are often too coarse, usually at 25 km spatial resolution (Gruhier et al., 2010), not suitable for the LST downscaling. A closer examination of the prediction errors suggests that urban pixels tended to yield greater prediction biases. The selected variables must be further investigated in terms of appropriateness for urban LST studies. Fig. 4 shows the observed GOES LSTs at 5 km, the predicted GOES LSTs at 1 km, and the observed MODIS LST measurements (1 km) at the same overpass time. Visually, the downscaled GOES LSTs captured the general patterns of LST over the study area quite well as compared with the MODIS observations.

4.2. DTC modeling results

Fig. 5 shows the modeling results for the shrubland and developed areas in different months. Compared with the original 5-km GOES LSTs, downscaled LSTs presented stronger diurnal fluctuations, especially after the nighttime attenuation started. This result suggested that the proposed downscaling method was more suitable for the daytime other than the nighttime due to the limited ability of the auxiliary data to reveal LST dynamics during the nighttime. In addition, the downscaled 1 km LSTs in the developed areas displayed larger fluctuations than those in the shrubland. The urban-shrubland difference in LST temporal variation prompted us to consider several factors in downscaling LSTs. First, the complexity of urban landscapes (forms and structures) tended to create more anomalies in LST. Moreover, the inconsistent LST diurnal variations at 5 km may be related to the uncertainty resulted from the application of the split window algorithm. The lack of available atmospheric profiles hindered the acquisition of split window regression coefficients through simulations. Instead, by collecting large amount of MODIS and GOES pixel pairs, split window regression coefficients could be derived. However, this kind of computation needs to assume that regression coefficients did not change over time. During the fitting processes, coefficients were derived by using all the pixels, thus neglecting possible local variations and changes caused by meteorological conditions. Eventually, biases resulted from the LST computations were propagated to the downscaling procedure (i.e., LSSVM), generating large diurnal fluctuations in the downscaled LSTs. Therefore, we proposed to use the DTC model to fit the downscaled LSTs derived from the LSSVM procedure and to consider the DTC modeled values as the final downscaling results, also referred as DTC-smoothed LST values. Fig. 6 showed the evolution of LSTs, which can also be used to examine the surface urban heat island (SUHI) at a temporal resolution of 30 min from 09:00 to 19:30 local time on August 12, 2005. The presented images were the products of DTC-smoothed LST at 1 km resolution. To ensure a consistent comparison, the same data classification scheme and color scale were applied to all the predicted LST images. Gradual changes in LST can be clearly seen. Further extraction of urban thermal parameters (such as UHI center, magnitude, and extent) would be promising and possible.

Table 1 provided the DTC modeling results and their differences at 1 km and 5 km for the selected urban and shrubland areas. The *fitted RMSE* in Table 1 quantified the fitting results and showed mostly large errors at 1 km, which unfolded that the downscaling LSTs, to some extent, deteriorated the original diurnal temperature variations. On 01/12/2005, there was small discrepancy in the modeling result between developed and shrubland sites. In fact, except for the parameter T_0 (i.e., minimum temperature around sunrise), other parameters of the model showed very similar values at both 1-km and 5-km resolutions. Thus, the "Fit 1–Fit 5" value (the difference between fitting results at 1 km and 5 km) was negative for both developed and shrubland sites. On 05/12/2005, shrubland illustrated a great difference in temperature amplitude (T_a). This was due to the reduction of the highest temperature at 1 km, which may be attributed to the prorogated errors from the split window algorithm. The minimum temperature around sunrise (T_0) was larger in the developed area than that in the shrubland. This is reasonable given the existence of anthropogenic heat discharge in the urban areas. On 08/12/2005, modeling parameters derived at 1 km and 5 km for shrubland were very close except for δT. The large value of divergence should be attributed to strong LST fluctuations resulted from the downscaling after the start of nighttime attenuation at 1 km. This should also be the reason why the fitted RMSE at 1 km was significantly larger than that at 5 km. In contrast, the developed land showed similar value of each parameter at both resolutions. On 10/15/2005, shrubland observed similar parameters at 1 km and 5 km except for T_a. The possible reason was the dampening of the highest temperature at 1 km resulted from LST downscaling process. Similar to 08/12/2005, the modeling parameters in October for the developed site did not show large differences at both resolutions. Although LSTs presented large fluctuations in both August and October, the DTC modeling process smoothed the troughs and peaks. For all months, in terms of fitted LSTs (Fit 1–Fit 5), it is suggested that downscaled LSTs had an accuracy of 0.1–2.2 K for shrubland and 0.2–1.5 K for developed area. Based on the analysis of all modeling results, it can be concluded that downscaled GOES LSTs at 1 km preserved well the diurnal temperature cycle and that the prediction accuracy was reasonably high (approximately 2.5 K for all the 48 images). The downscaled LSTs smoothed by DTC preserved the vast majority of information of LST diurnal dynamics.

5. Discussion

The performance of the proposed disaggregation procedures was principally dependent upon the quality of auxiliary datasets. Prediction errors originated from the up-scaling process, especially over heterogeneous regions, such as developed areas. The up-scaling process, indeed, averaged the variations of LST associated parameters from 1 km to 5 km, resulting in the loss of local variance and thus leading to large errors. In addition, the matching of MODIS 1-km pixels to GOES 5-km pixels inevitably introduced some geo-location errors. Another aspect that influenced the downscaling processes would be the application of split window algorithm to derive GOES LSTs by fitting matched MODIS and GOES pixel pairs to estimate regression coefficients. The basic assumption was that there were not any changes in the coefficients, neglecting local variations and meteorological conditions that could impact the regression coefficients.

Fig. 6 shows that predicted 1-km LSTs exhibited more fluctuations over successive sunrises, which may suggest the combined impact of the downscaling procedure and the derivation of LST from GOES image data. A better way to derive GOES LSTs should be based on the MODTRAN model to simulate the regression coefficients by using appropriate atmospheric parameters. Due to the unavailability of crucial atmospheric data this study had to collect substantial amount of MODIS and GOES pixel-pairs, making it possible to employ the least square regression (LSR) to compute the split window coefficients (Inamdar et al., 2008). The optimization of LSR would allow for the computation for all collected pixel-pairs globally and neglecting specific atmospheric conditions for a particular day. Another potential source of error in the prediction may be related to the incomplete inclusion of factors contributing to LST variations. For example, soil moisture may be an important factor influencing LST variations in an arid or semi-arid environment such as Los Angeles.

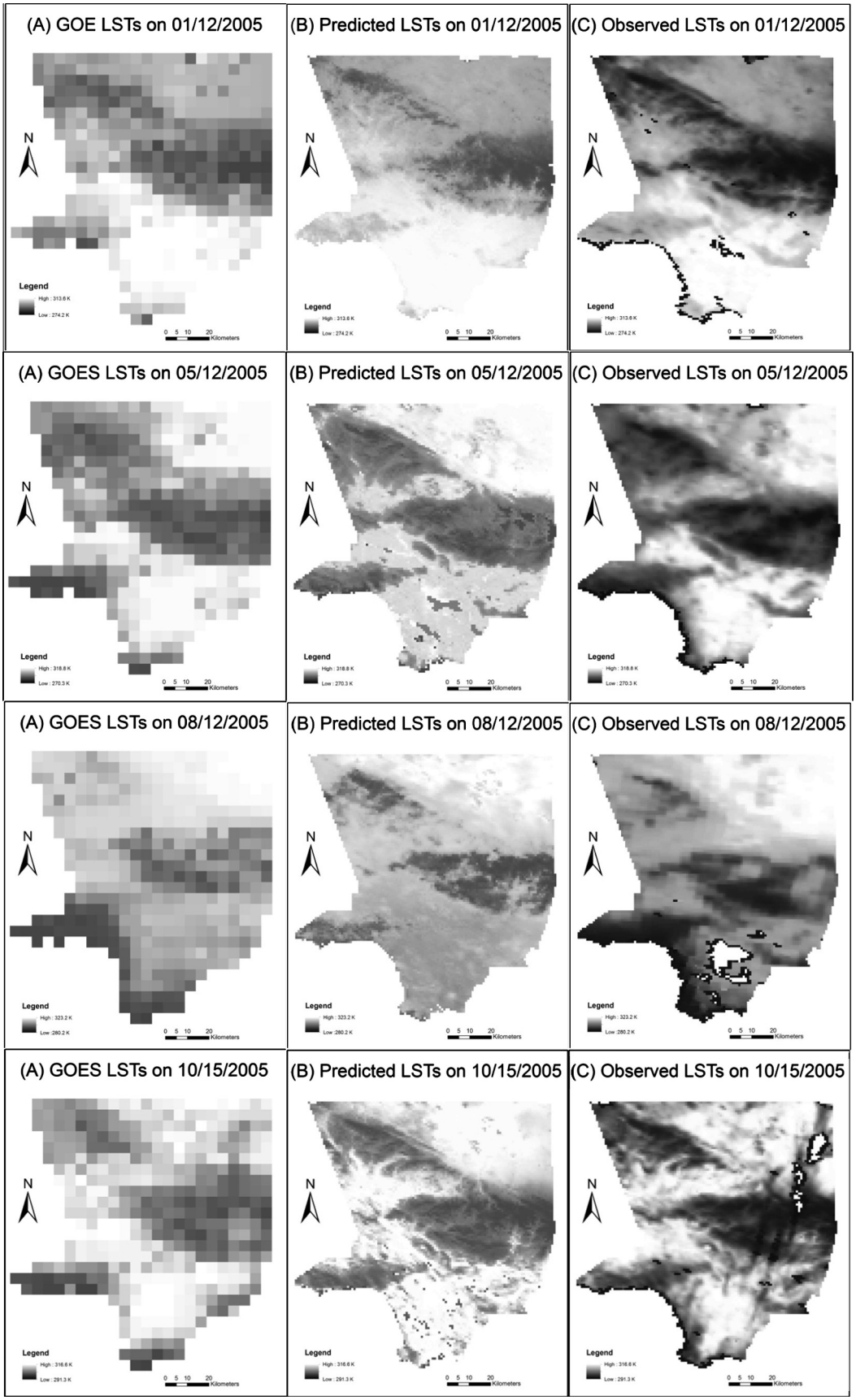

Fig. 4. The observed GOES LSTs at 5 km resolution (Panel A), the predicted LSTs at 1 km resolution (Panel B), and the observed MODIS LST measurements at 1 km at the same overpass time (Panel C) on January 12, May 12, August 12 and October 15, 2005. Gaps in the Panel C were removed according to the QA layer of the MODIS product.

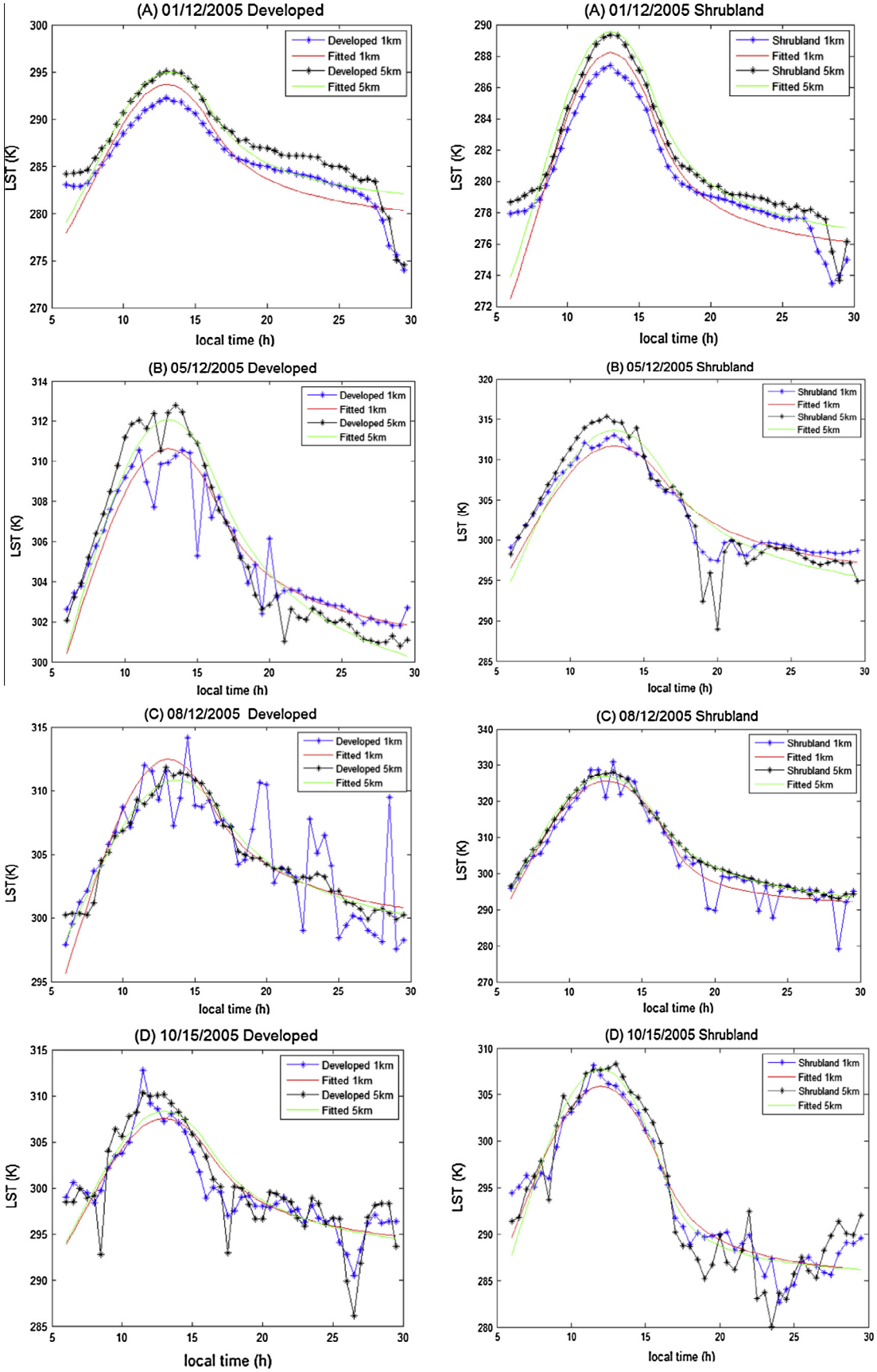

Fig. 5. DTC modeling results for shrubland (Left) and developed (Right) on (A) 01/12, (B) 05/12, (C) 08/12, (D) 10/15, 2005. 1-km LSTs were extracted from the downscaled GOES images and 5 km LSTs were derived from the GOES images. The *x*-axis represents local time from 6 am to 6 am next day (30 h). Fitted 1 km and 5 km means the DTC modeled results at 1 km and 5 km.

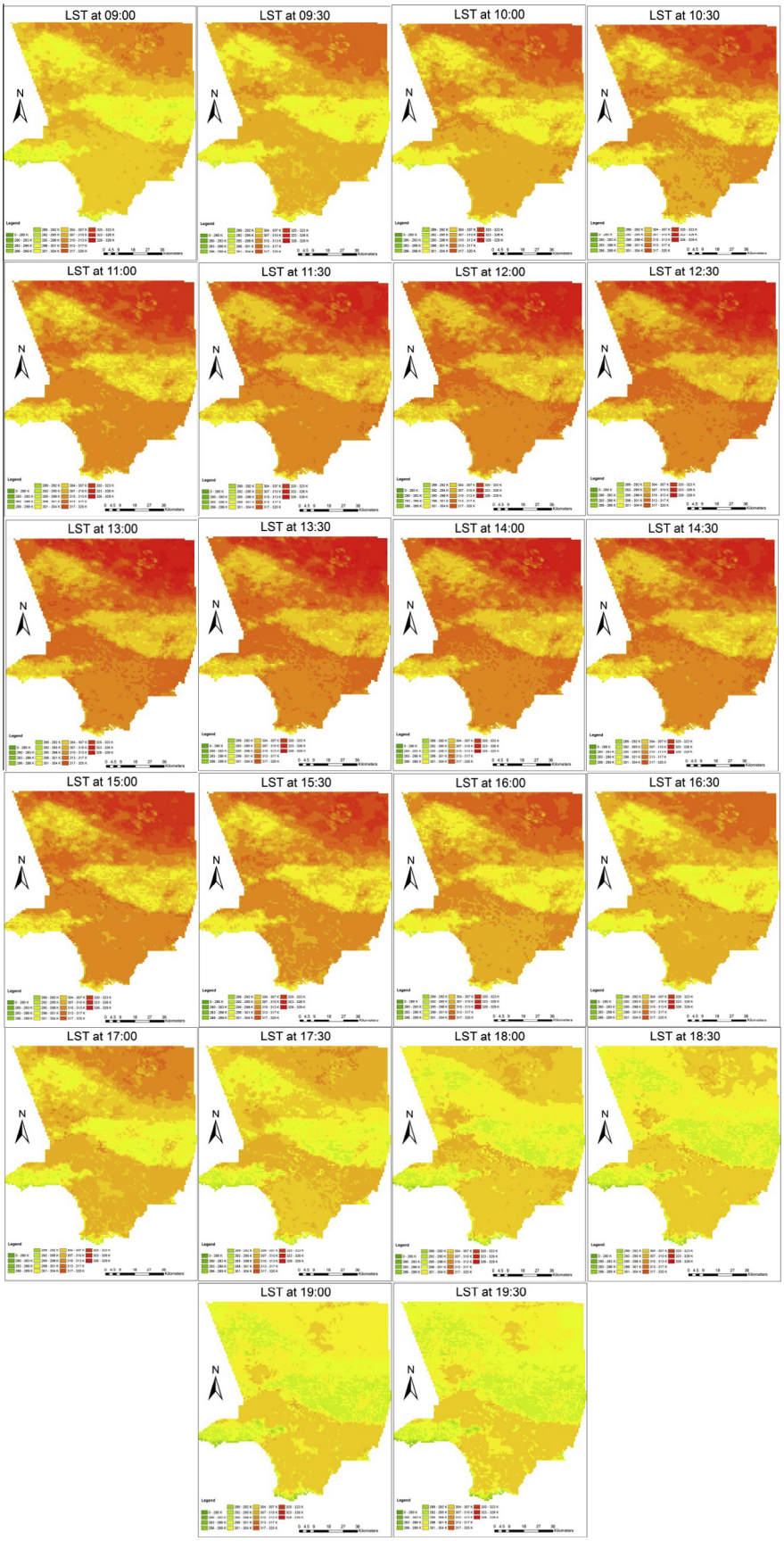

Fig. 6. Evolutions of LST pattern from 09:00 to 19:30 (local time) in Los Angeles on August 12, 2005.

Table 1
Statistics of the DTC modeling results for selected shrubland and developed areas.

Date	Land cover	Resolution	T_0 (K)	T_a (K)	ω (h)	T_m (h)	T_s (h)	k	δT (K)	Fitted RMSE	Fit 1–Fit 5 (mean/RMSE)
Jan	Shrubland	1 km	278.2	10.3	10.1	13.5	17.1	3.5	−4.0	1.4	−1.2/0.2
		5 km	279.5	10.1	10.3	13.3	17.2	3.7	−4.7	1.2	
	Developed	1 km	283.6	10.5	10.1	13.0	17.1	5.3	−6.1	2.0	−1.5/0.2
		5 km	285.0	10.4	10.1	13.1	17.0	4.3	−5.7	2.1	
May	Shrubland	1 km	297.4	14.3	13.5	13.2	18.7	1.3	0.1	1.1	0.1/1.4
		5 km	296.0	17.7	13.5	13.6	18.6	1.2	0.4	2.4	
	Developed	1 km	300.9	10.0	13.8	13.1	18.3	1.0	1.5	1.1	−0.2/1.0
		5 km	301.9	10.2	13.5	13.2	18.5	1.9	−1.4	0.7	
Aug	Shrubland	1 km	296.7	25.6	13.3	12.5	17.3	3.7	−4.9	3.7	−2.2/1.5
		5 km	298.9	25.4	13.4	12.5	17.3	3.7	3.7	0.8	
	Developed	1 km	297.7	15.0	13.3	13.4	17.3	2.4	−4.2	3.0	0.2/0.5
		5 km	297.5	15.1	13.5	13.5	17.2	2.4	−4.5	1.3	
Oct	Shrubland	1 km	291.5	14.5	11.1	12.5	16.5	2.9	−7.4	1.9	−0.1/0.9
		5 km	290.0	17.8	11.3	12.4	16.5	2.2	−5.2	2.8	
	Developed	1 km	297.5	10.1	11.3	13.0	16.4	5.1	−6.0	2.4	−0.3/0.4
		5 km	298.2	10.2	11.1	13.0	16.5	5.5	−7.6	3.0	

Note: (1) DTC modeling parameters: minimum temperature around sunrise (T_0), temperature amplitude (T_a), length of daylight hours (ω), time of maximum (T_m), start of nighttime attenuation (T_s), attenuation coefficient (k), and δT at 1 km and 5 km.
(2) Fitted root mean square error (RMSE) quantified the accuracy of DTC fitting result.
(3) The last column (Fit 1–Fit 5) shows the difference between the DTC fitting results at 1 km and 5 km.
(4) The dates were for 01/12, 05/12, 08/12, and 10/15, 2005, respectively.

The DTC model by Inamdar et al. (2008) employed a harmonic and a decay function to describe diurnal temperature variations. A debatable point is its suitability for characterizing the nighttime attenuation and the LST variability around the sunrise time. Therefore, other models have been developed to simulate nighttime and daytime variations. For example, Gottsche and Olesen (2009) developed a DTC model by incorporating the optical thickness parameter on the basis of extraterrestrial solar irradiation and the energy balance of the land surface. The system of equations (as proposed by Gottsche and Olesen, 2009) has been demonstrated to be able to better simulate both the variations of LST around sunrise and the natural variability of DTC width and slope. Since this study employed a DTC model to smooth the downscaled LSTs, further comparisons between various DTC models were not conducted. Our primary interest was the comparisons of different parameters (e.g., temperature amplitude, minimum temperature around sunrise) derived at varied spatial scales. Further, Inamdar et al. (2008) and Inamdar and French (2009) applied the DTC model to the median-composite LSTs in order to fill the gaps caused by cloud contamination. This procedure was not adopted in this study because it may introduce additional uncertainty. The DTC estimated from a long-term trend that in reality cannot portrait the impacts of cloud contamination or rainfall events occurred at short-term time scales, deviating from the actual diurnal cycle of LST.

Fig. 5 showed that DTC varied with LULC type. For the present study, we chose only two land covers (i.e., shrubland and developed area) for the DTC analysis, because a homogeneous pixel (5 km by 5 km) for other LULC types was not possible to extract. Possible causes for the observed differences in DTC among land covers were soil moisture, evapotranspiration, and vegetation. High soil moisture, evapotranspiration, and vegetation during daytime can reduce the maximum temperature and hence lead to distinct temporal trends. The integration of these parameters may have large impacts on the temporal dynamics of LSTs, especially in the arid and semiarid environments. This was evident from decreased temperature amplitude in the developed area given the fact that urbanization was largely realized through the replacements of natural surfaces (e.g., shrubland) with impervious surfaces. The creation of impervious surfaces changes surface energy balance (Weng et al., 2004; Carlson 2007; Anderson et al., 2012). Further investigations should be conducted on the impact of soil moisture, evapotranspiration, and vegetation on the diurnal temperature dynamics with various land covers.

6. Conclusions

This study aimed at exploring an efficient and effective way to downscale half-hourly GOES LSTs from 5 km to 1 km spatial resolution for investigations of environmental issues, such as urban heat island monitoring and heat risk assessments. The result demonstrated that the proposed LSSVM method can achieve this goal successfully with the predicted accuracy around 2.5 K, when validated against MODIS LST measurements at the same overpass time. The availability of auxiliary datasets, including vegetation indexes, elevation data, albedo, and emissivity, enabled frequent estimation of LST and thus its diurnal cycle. In the process of fusing GOES and MODIS data, a series of analytical steps were implemented, including BTH cloud screening, LST estimating with the split-window scheme, up-scaling of auxiliary datasets to 5 km, disaggregation with LSSVM, and validation with MODIS measurements. However, main errors resulted from the derivation of GOES LSTs, aggregation of the auxiliary datasets to match the GOES pixels, and reliability of emissivity data product. Further extraction of DTC parameters from the fused datasets suggested that the DTC smoothed downscaled images yielded an accuracy of 0.1–2.2 in terms of fitted LSTs at 1 km and 5 km.

The principle innovation of this research is that it provides synthetic half-hourly 1-km LST data suitable for analysis of DTC dynamics. Previous studies have shown the accuracy of downscaled GOES LST data can reach approximately at 2.5 K (Inamdar et al., 2008; Zakšek and Oštir, 2012; Keramitsoglou et al., 2013); however, the use of downscaled images for time sequential analysis was limited and their value for diurnal temperature modeling was not fully recognized. This study investigated the usefulness of the downscaled 1-km LSTs to extract DTC parameters. Moreover, this research can overcome the gaps caused by cloud contamination as long as cloud contaminated pixels did not affect the training procedure of LSSVM. For regions experiencing more cloudy days, new methods should be developed to model LST temporal variations and to assess the impact of cloud cover (Weng and Fu, 2014).

The proposed method can be extended to derive half-hourly LSTs at higher spatial resolution when appropriate auxiliary

datasets are available. For example, MODIS data products offer vegetation indices at 250 m and 500 m resolutions. Therefore, it is theoretically possible to downscale GOES images to the spatial resolution of 250 or 500 m. Nevertheless, the involved scale issues must be examined in details since LST is spatially heterogeneous, especially over the urban areas. Because of the lack of real LST measurements at 250 or 500 m resolution, methods for validating modeling results should also be developed.

References

Anderson, M.C., Allen, R.G., Morse, A., Kustas, W.P., 2012. Use of Landsat thermal imagery in monitoring evapotranspiration and managing water resources. Remote Sens. Environ. 122, 50–65.

Buscail, C., Upegui, E., Viel, J.F., 2012. Mapping heatwave health risk at the community level for public health action. Int. J. Health Geographics 11, 38. http://dx.doi.org/10.1186/1476-072X-11-38.

Carlson, T., 2007. An overview of the "triangle method" for estimating surface evapotranspiration and soil moisture from satellite imagery. Sensors 7 (8), 1612–1629.

Dominguez, A., Kleissl, J., Luvall, J.C., Rickman, D.L., 2011. High-resolution urban thermal sharpener (HUTS). Remote Sens. Environ. 115 (7), 1772–1780.

Duan, S.B., Li, Z.L., Wang, N., Wu, H., Tang, B.H., 2012. Evaluation of six land-surface diurnal temperature cycle models using clear-sky in situ and satellite data. Remote Sens. Environ. 124, 15–25.

Friedl, M.A., 2002. Forward and inverse modeling of land surface energy balance using surface temperature measurements. Remote Sens. Environ. 79 (2–3), 344–354.

Fry, J., Xian, G., Jin, S., Dewitz, J., Homer, C., Yang, L., Barnes, C., Herold, N., Wickham, J., 2011. Completion of the 2006 National Land Cover Database for the Conterminous United States. PE&RS 77 (9), 858–864.

Gottsche, F.M., Olesen, F.S., 2001. Modelling of diurnal cycles of brightness temperature extracted from METEOSAT data. Remote Sens. Environ. 76 (3), 337–348.

Gottsche, F.M., Olesen, F.S., 2009. Modelling the effect of optical thickness on diurnal cycles of land surface temperature. Remote Sens. Environ. 113 (11), 2306–2316.

Gruhier, C., de Rosnay, P., Hasenauer, S., Holmes, T., de Jeu, R., Kerr, Y., Mougin, E., Njoku, E., Timouk, F., Wagner, W., Zribi, M., 2010. Soil moisture active and passive microwave products: intercomparison and evaluation over a Sahelian site. Hydrol. Earth Syst. Sci. 14 (1), 141–156.

Guo, L.J., Moore, J.M., 1998. Pixel block intensity modulation: adding spatial detail to TM band 6 thermal imagery. Int. J. Remote Sens. 19 (13), 2477–2491.

Harlan, S.L., Brazel, A.J., Prashad, L., Stefanov, W.L., Larsen, L., 2006. Neighborhood microclimates and vulnerability to heat stress. Soc. Sci. Med. 63 (11), 2847–2863.

Inamdar, A.K., French, A., 2009. Disaggregation of GOES land surface temperatures using surface emissivity. Geophys. Res. Lett. 36, L02408. http://dx.doi.org/10.1029/2008GL036544.

Inamdar, A.K., French, A., Hook, S., Vaughan, G., Luckett, W., 2008. Land surface temperature retrieval at high spatial and temporal resolutions over the southwestern United States. J. Geophys. Res. – Atmos. 113, D07107. http://dx.doi.org/10.1029/2007JD009048.

Jedlovec, G.J., Laws, K., 2003. GOES cloud detection at the Global Hydrology and Climate Center. Preprints, 12th Conf. on Satellite Meteorology and Oceanography, Long Beach, CA, Amer. Meteor. Soc., CD-ROM, P1.21.

Jeganathan, C., Hamm, N.A.S., Mukherjee, S., Atkinson, P.M., Raju, P.L.N., Dadhwal, V.K., 2011. Evaluating a thermal image sharpening model over a mixed agricultural landscape in India. Int. J. Appl. Earth Obs. Geoinf. 13 (2), 178–191.

Karl, T.R., Kukla, G., Gavin, J., 1984. Decreasing Diurnal Temperature Range in the United States and Canada from 1941 through 1980. J. Climate Appl. Meteorol. 23 (11), 1489–1504.

Keramitsoglou, I., Kiranoudis, C.T., Weng, Q., 2013. Downscaling GOEStationary land surface temperature imagery for Urban analysis. IEEE Geosci. Remote Sens. Lett. 10 (5), 1253–1257.

Kustas, W.P., Norman, J.M., Anderson, M.C., French, A.N., 2003. Estimating subpixel surface temperatures and energy fluxes from the vegetation index-radiometric temperature relationship. Remote Sens. Environ. 85 (4), 429–440.

Lafortezza, R., Carrus, G., Sanesi, G., Davies, C., 2009. Benefits and well-being perceived by people visiting green spaces in periods of heat stress. Urban Forest. Urban Green. 8 (2), 97–108.

Mantero, P., Moser, G., Serpico, S.B., 2005. Partially supervised classification of remote sensing images through SVM-based probability density estimation. IEEE Trans. Geosci. Remote Sens. 43 (3), 559–570.

Merlin, O., Duchemin, B., Hagolle, O., Jacob, F., Coudert, B., Chehbouni, G., Dedieu, G., Garatuza, J., Kerr, Y., 2010. Disaggregation of MODIS surface temperature over an agricultural area using a time series of Formosat-2 images. Remote Sens. Environ. 114 (11), 2500–2512.

Mountrakis, G., Im, J., Ogole, C., 2011. Support vector machines in remote sensing: a review. ISPRS J. Photogram. Remote Sens. 66 (3), 247–259.

Oke, T.R., 1982. The energetic basis of the urban heat island. Quart. J. Royal Meteorol. Soc. 108 (455), 1–24.

Oke, T.R., Zeuner, G., Jauregui, E., 1992. The surface-energy balance in Mexico-City. Atmos. Environ. Part B – Urban Atmos. 26 (4), 433–444.

Owen, T.W., Carlson, T.N., Gillies, R.R., 1998. An assessment of satellite remotely-sensed land cover parameters in quantitatively describing the climatic effect of urbanization. Int. J. Remote Sens. 19 (9), 1663–1681.

Pu, R.L., Gong, P., Michishita, R., Sasagawa, T., 2006. Assessment of multi-resolution and multi-sensor data for urban surface temperature retrieval. Remote Sens. Environ. 104 (2), 211–225.

Rajasekar, U., Weng, Q., 2009. Urban heat island monitoring and analysis using a non-parametric model: A case study of Indianapolis. ISPRS J. Photogram. Remote Sens. 64 (1), 86–96.

Shi, W.Z., Zheng, S., Tian, Y., 2009. Adaptive mapped least squares SVM-based smooth fitting method for DSM generation of LIDAR data. Int. J. Remote Sens. 30 (21), 5669–5683.

Streutker, D.R., 2003. Satellite-measured growth of the urban heat island of Houston, Texas. Remote Sens. Environ. 85 (3), 282–289.

Sun, D.L., Pinker, R.T., Kafatos, M., 2006. Diurnal temperature range over the United States: a satellite view. Geophys. Res. Lett. 33, L05705. http://dx.doi.org/10.1029/2005GL024780.

Tomlinson, C.J., Chapman, L., Thornes, J.E., Baker, C.J., 2011. Including the urban heat island in spatial heat health risk assessment strategies: a case study for Birmingham, UK. Int. J. Hea. Geogr 10, 42.

Van De Kerchove, R., Lhermitte, S., Veraverbeke, S., Goossens, R., 2013. Spatio-temporal variability in remotely sensed land surface temperature, and its relationship with physiographic variables in the Russian Altay Mountains. Int. J. Appl. Earth Obs. Geoinf. 20, 4–19.

Wan, Z.M., Dozier, J., 1996. A generalized split-window algorithm for retrieving land-surface temperature from space. IEEE Trans. Geosci. Remote Sens. 34 (4), 892–905.

Weinreb, M., Jamieson, M., Fulton, N., Chen, Y., Johnson, J.X., Bremer, J., Smith, C., Baucom, J., 1997. Operational calibration of GOEStationary operational environmental satellite-8 and -9 imagers and sounders. Appl. Opt. 36 (27), 6895–6904.

Weng, Q., Fu, P., 2014. Modeling annual parameters of land surface temperature variations and evaluating the impact of cloud cover using time series of Landsat TIR data. Remote Sens. Environ. 140, 267–278.

Weng, Q., Fu, P., Gao, F., 2014a. Generating daily land surface temperature at Landsat resolution through fusing Landsat and MODIS data. Remote Sens. Environ. 145, 55–67.

Weng, Q., Hu, X., Quattrochi, D.A., Liu, H., 2014b. Estimating seasonal changes in urban surface heat fluxes by using ASTER images and routine meteorological data. IEEE J. Select. Topics Appl. Earth Observations Remote Sens.. http://dx.doi.org/10.1109/JSTARS.2013.2281776.

Weng, Q.H., Lu, D.S., Schubring, J., 2004. Estimation of land surface temperature-vegetation abundance relationship for urban heat island studies. Remote Sens. Environ. 89 (4), 467–483.

Zakšek, K., Oštir, K., 2012. Downscaling land surface temperature for urban heat island diurnal cycle analysis. Remote Sens. Environ. 117, 114–124.

Zheng, S., Shi, W.Z., Liu, H., Tian, J.W., 2008. Remote sensing image fusion using multiscale mapped LS-SVM. IEEE Trans. Geosci. Remote Sens. 46 (5), 1313–1322.